

PLX Latchup Tests, 19-20 October 2014

Contact:

Michal Szelezniak
Leo Greiner
Giacomo Contin
Jo Schambach

Test goals	1
Test environment	2
Test setup	2
Devices under test	2
Hardware	3
Software	6
Test Results	6
Heavy Ions	6
Protons	10
Summary	10
Notes and Observations	12
Appendix A	13
Appendix B	16

Test goals

The goals of these tests were to try to reproduce the damage seen in the PXL detector during the RHIC run 14, to describe the failure mechanism and to define a safe operation envelope of latch-up current threshold settings to operate the PXL detector in the STAR 2015 run. The damage observed in the PXL detector during the initial phase of the physics run manifested itself in increased digital current consumption in the affected ladders and partial or full loss of detection capabilities in pixel sub-arrays and whole sensors¹. The damage rate was successfully reduced using operational methods, especially by lowering the over-current threshold on the digital power supplies from 400 mA to 120 mA above the operating current (~800 mA) and limiting the detector exposure to radiation. A working assumption that could explain the observed damage was that the damage was induced by latch-up or latch-up-like events.

General latch-up tests that were performed on silicon sensors during the development of the PXL detector did not result in any permanent damage in the tested devices. However, those tests were performed on full thickness, single sensors featuring low-resistivity epitaxial layer². The sensors used in the PXL detector are 50 μm thin, feature high-resistivity epitaxial layer, and are grouped into 10-sensor ladders.

¹ L.Greiner et al., "Experience from Construction and Operation of the STAR PXL MAPS Based Vertex Detector", PIXEL 2014.

² http://rnc.lbl.gov/hft/hardware/docs/latchup/LU_SEU_2011.pdf

In this document we describe a series of latch-up test that we have prepared and conducted with a specific goal of testing production sensors and ladders to determine if latch-up events can lead to permanent damage in the silicon sensors used in the PXL detector as observed during the RHIC run 14.

Test environment

The tests were performed at the BASE facility³ at the 88" cyclotron, LBNL. One of the main advantages of this facility is the availability of a wide range of heavy ion beams and high-flux proton beams.

In this test we were mostly interested in studying sensor behavior in response to latch-up events at different over-current thresholds but we also wanted to compare the new and older latch-up cross-section measurements. For this reason we limited our tests to just two ion species selected from the 10 MeV/nucleon cocktail:

1. Ar at 9.74 MeV/(mg/cm²) for most of the measurements with varying thresholds
2. Ne at 3.49 MeV/(mg/cm²) for a few tests to compare with previous cross-section measurements

Argon was chosen as the main ion based on the previous test results that showed a latchup rate of 10 events per minute for the flux of $\sim 5e3$ /cm²/s. At this rate we expected to achieve reasonable statistics in the time allocated for the test.

In addition to heavy ions, we planned on exposing PXL sensors to 50 MeV protons. Based on the related literature, the expected LU cross-sections for protons are a few orders of magnitude lower than for heavy ions.

Initially the tests were scheduled for a single 28-hour block starting on October 19 during which we expected to run tests using heavy ion and proton beams. Eventually, the higher priority heavy ion tests yielded very interesting results and consumed all the allocated time. Due to an unexpected opening in the cyclotron schedule, we were also given an 8-hour window for tests with a proton beam on October 28.

Taking into account the time spent on beam tuning and handling of test devices and the associated operation of the vacuum chamber, the integrated exposure time to heavy ion beams was approximately 10.5 hrs. Similarly, the integrated exposure time to the proton beam was just under 3 hrs.

Test setup

Heavy ions tests at the BASE facility are conducted in vacuum (Cave 4B) while proton beam exposures are conducted in air (Cave 4A). The test setup configuration was very similar for both heavy ion and proton tests.

Devices under test

Heavy ion running:

- 2 x newly constructed PXL ladder
- 2 x thinned (50 um) high-resistivity epi sensors on individual testing PCB
- 1 x thick (700 um) high-resistivity epi sensor on an individual testing PCB

³ <http://cyclotron.lbl.gov/base-rad-effects>

- 1 x thick (700 um) low-resistivity epi sensor on an individual testing PCB
- Test structures for IPHC⁴

The tests structures were attached to mounting plates as shown in Figure 1. These plates were placed into contact with a cooling plate that was mounted to the exposure plate in the vacuum tank. Two ladders and 4 individual sensors were divided into three independent test sets.

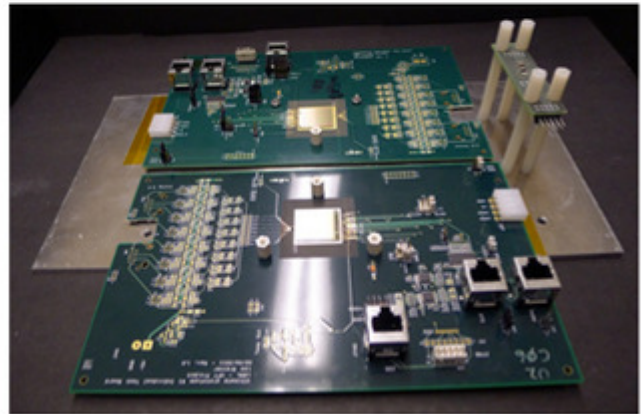
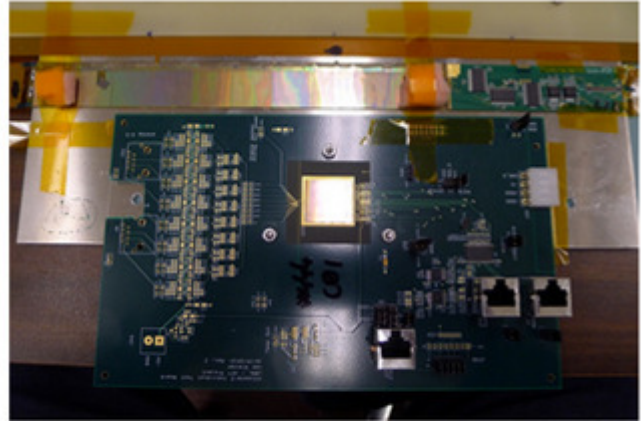
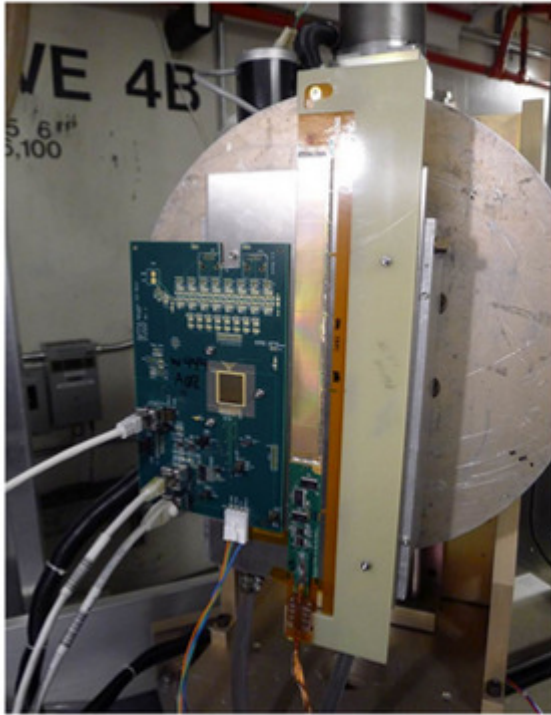


Figure 1 Mounting of the test structures for tests with heavy-ions beams. A) A single sensor and a PXL ladder attached to a cooling plate and the test station in the vacuum tank. B) The second test setup composed of a single sensor and a PXL ladder. C) The third setup consisted of two individual sensors and two small dedicated LU test chips from IPHC mounted on large standoffs.

Proton running:

- 1 newly constructed PXL ladder
- 1 x thick (700 um) high-resistivity epi sensor on an individual testing PCB

Both test devices were attached to the same plate in the same way as for heavy ion tests.

Hardware

The test setup consisted of a basic unit of the PXL detector readout system – one main PXL readout board (RDO) and one mass-termination board (MTB). The only modification between the complete PXL readout system and the setup for latch-up tests is the addition of adapter boards that provide connections through the standard vacuum chamber flanges (IDC connectors). Both proton and heavy ion tests used the same connections as is shown in Figure 2. These

⁴ The test results obtained on these structures are beyond the scope of this report.

adapter boards connect the ladder under test to the Ladder1 path in the MTB and the individual sensor under test to the Ladder2-Sensor1 data path. This approach allowed us to have two devices available for testing inside the vacuum chamber and therefore reduced the number of vacuum chamber access cycles. It also allowed us to test a ladder and a single sensor at the same time during proton beam exposures.

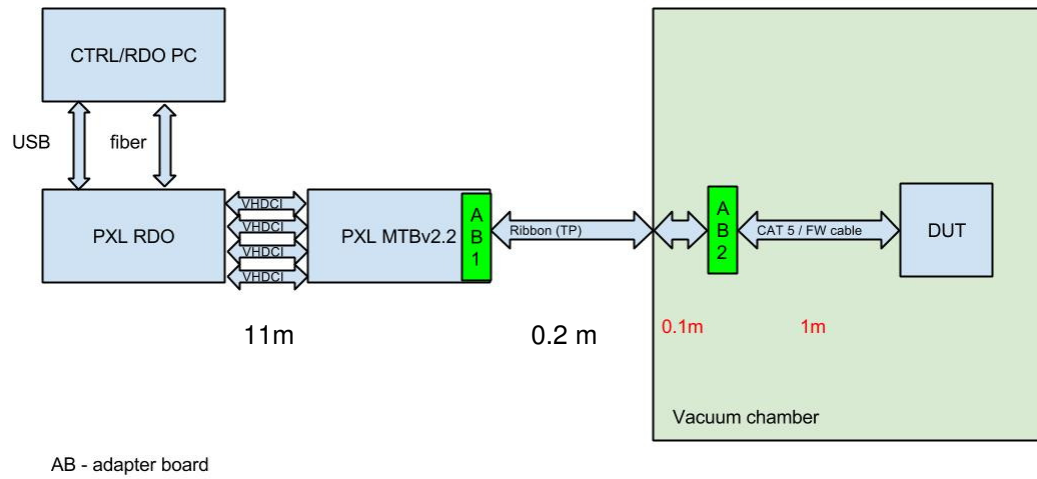


Figure 2 Diagram of the test setup.

The control/readout PC and the PXL RDO board were located in the control shack outside of the testing cave. The setup in the cave was limited to devices under test (DUTs), the MTB and associated power supplies.

Figure 3 and Figure 4 show pictures of the test setup in Cave 4B and inside the vacuum chamber.

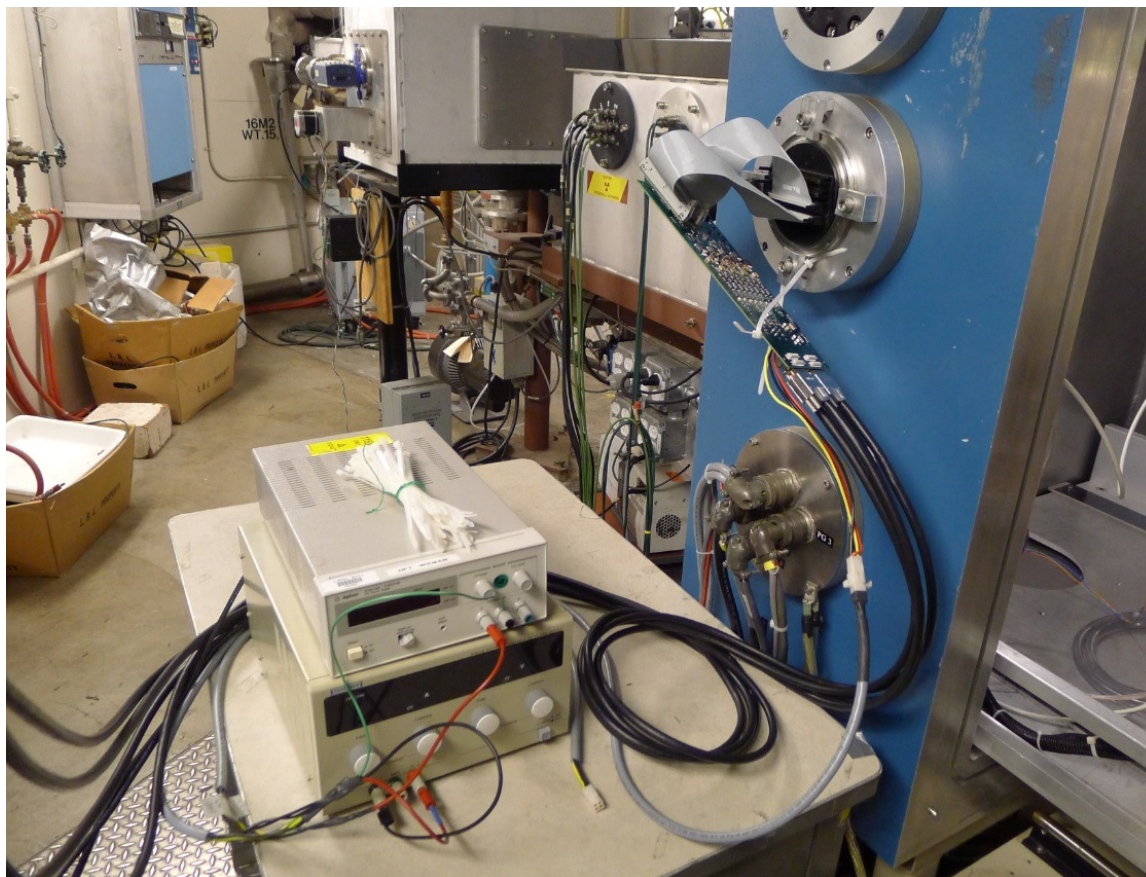


Figure 3 Test setup in Cave 4B. The PXL mass termination board (MTB) can be seen attached close to the chamber flange connectors. The power supplies set on the bench power the MTB.

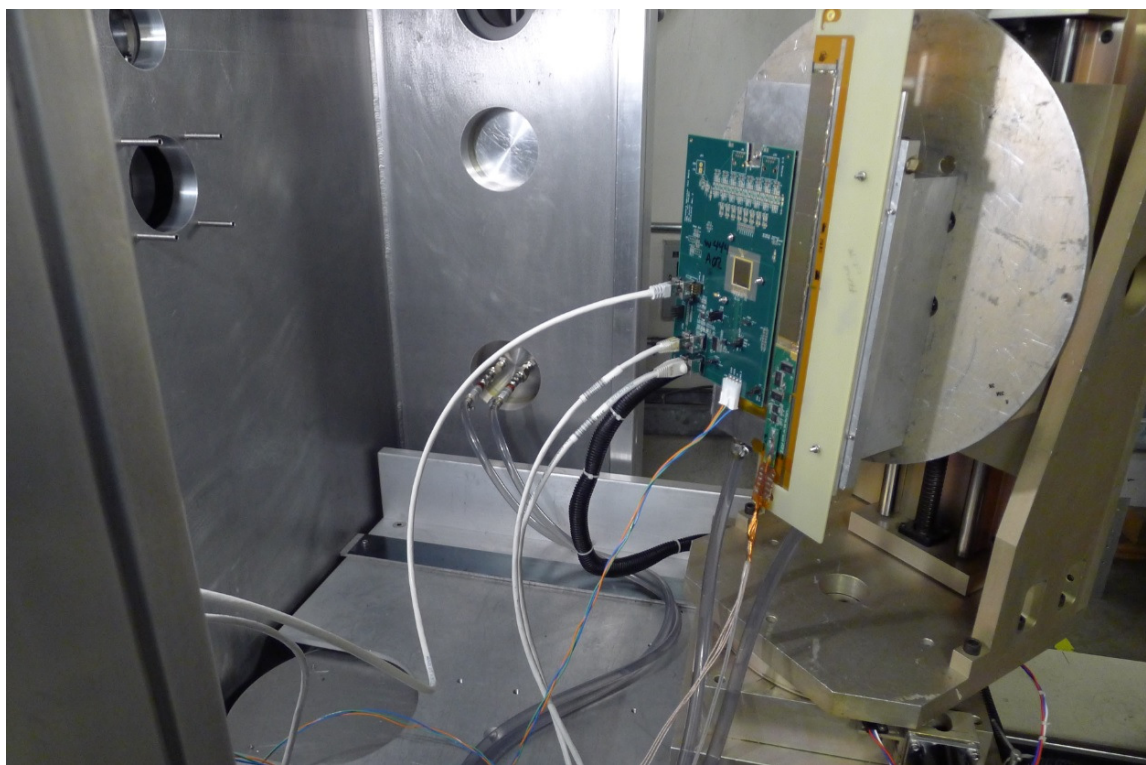


Figure 4 Test setup in vacuum chamber in Cave 4B. CAT5 connections to the individual sensor board and fine wire cable connecting the PXL ladder are visible in the foreground.

Software

The LU monitoring and data acquisition system was basically the same as the one built into the PXL detector readout. In this system, LU events are automatically detected counted, and a full “LU recovery procedure” (explained below) is executed, while the LU counters can be read out through the PXL RDO USB interface.

The readout system for LU tests featured one important modification compared to the original system. The current monitoring ADC located on the MTB was readout continuously⁵ and the resulting ADC data was embedded into the PXL event structure. The internal periodic event trigger was set slow enough to limit the overall data flow⁶ and, at the same time fast enough to avoid overflowing the dedicated buffer used for storing data from the current monitoring ADC. This allowed us to register and analyze the evolution of the current consumption in our DUTs.

Test Results

Heavy Ions

Both ladder prototypes became damaged and inoperable when exposed to the vacuum, as explained in Notes and Observations, and therefore did not provide any test results.

All four individual sensors were successfully tested and the test results are summarized in Figure 5. The two thin sensors were tested with over-current levels ranging from 120 mV up to 1.0 and 1.8 A above the original operating current. The thick sensors were tested with over-current thresholds from 300 mA to 2 A above the original operating current. Throughout this report all over-current thresholds are estimated with respect to the original operating currents before DUTs developed any damage. During these tests the sensors registered hundreds of LU events as shown in Table 1. The data points in Figure 5 take into account the dead time associated with LU recovery and are corrected for incompletely cleared latch-ups that lead to double counting (see Appendix A).

Both of the thin sensors started exhibiting permanent current consumption increase as soon as they were tested with over-current threshold set to or above 1 A. This current increase is consistent with the damage observed in the PXL detector. The thick sensors did not exhibit this behavior.

⁵ The maximum ADC sampling rate in our test setup is 5 kHz. During tests with heavy ions we monitored two channels (analog and digital power supply) with the sampling rate of 2.5 kHz each. Tests with protons required monitoring of 4 channels (analog and digital power for each of the two DUTs tested in parallel), which resulted in the channel sampling rate of 1.25 kHz.

⁶ For this test the sensors were configured similarly to the PXL detector configuration with the internal signal thresholds set to $\sim 5 \times \text{noise}$.

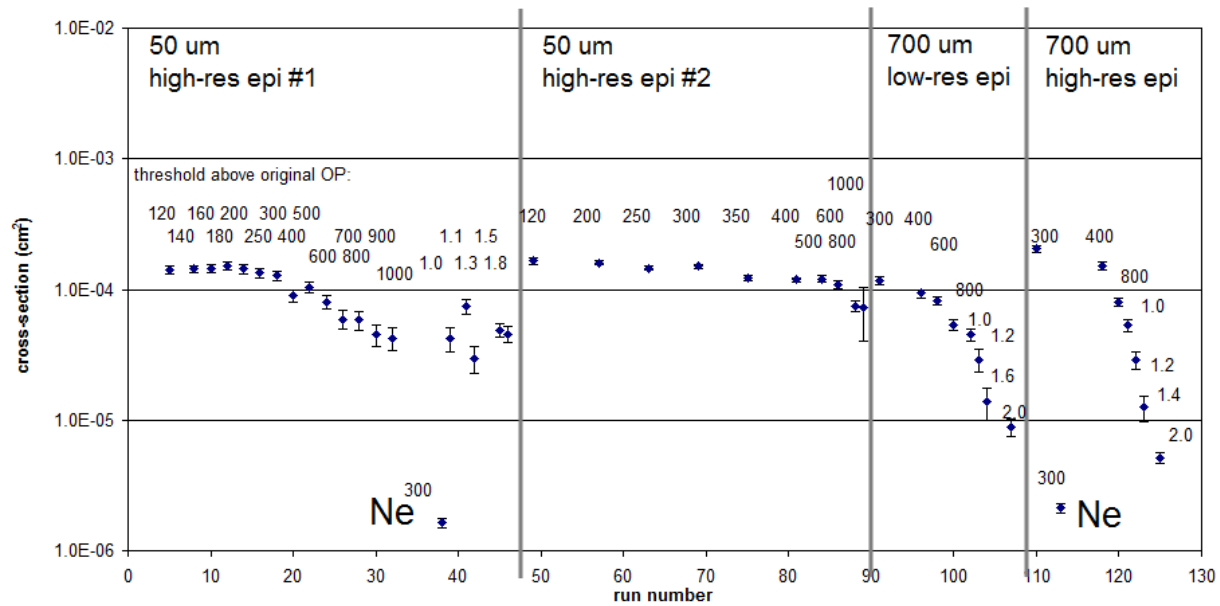


Figure 5 Summary of latch-up cross-sections for heavy ions measured for individual sensors as a function of the run number and the over-current threshold level.

Chip	LU count below 1A threshold	LU count at and above 1A threshold
1	1754	237
2	4439	5
3	652	43
4	817	248

Table 1 LU count for all 4 sensors tested with heavy ions.

The LU cross-sections measured in these tests agree within a factor of 2 with the results from the tests performed in 2011. It appears that the cross-sections measured for the sensors with high-res epitaxial layer are higher than the ones for low-res epi. However, the difference appears minimal and for the sake of this comparison it can be said that the two types of the epitaxial layer yield comparable results.

The drop in the cross-section measured for higher over-current threshold values is explained by the fact that the LU events observed in this testing session were current limited. This means that as the over-current limit was raised, we could accumulate more than one LU event in the sensor before exceeding the over-current limit that would trigger a proper LU recovery response.

Figure 6 shows the DUT current consumption during the LU recovery procedure. Different current levels are associated with power restoration, JTAG configuration of the sensor, restoration of the clock signal, and the final state with the sensor fully operating after it received the START signal. The default digital power consumption of 220 mA is a sum of the current drawn by the sensor and all of the on-board buffers that use the same power supply.

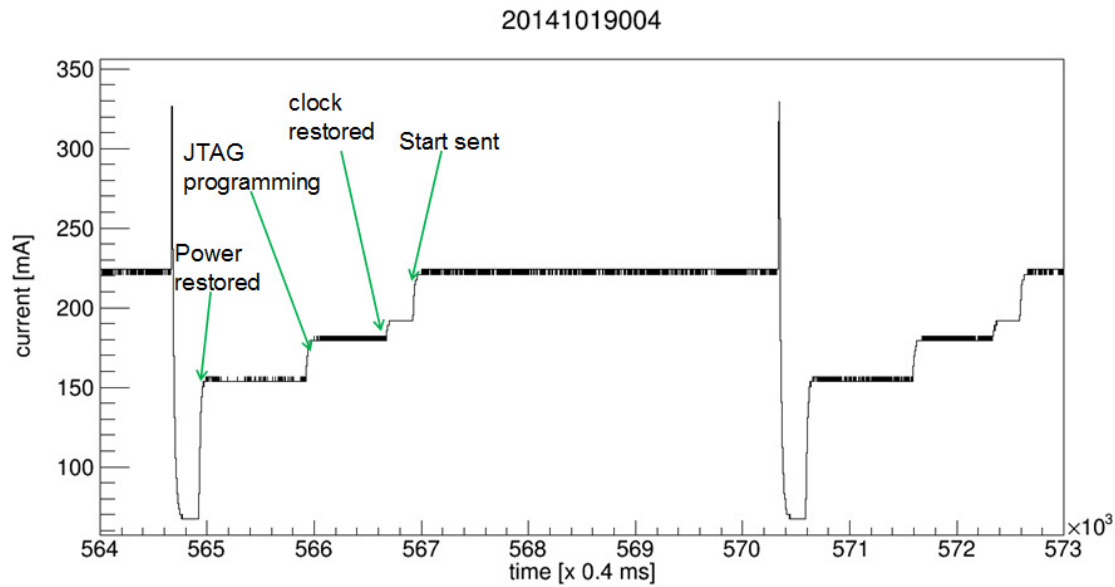


Figure 6 LU recovery profile with various stages of the sensor re-initialization.

Visual inspection of the current evolution in selected runs shows that sequential events, interpreted as current-limited latch-up, lead to a stable, increased current consumption that can exhibit quantized steps, example in Figure 7 A, or a more random pattern, as shown in Figure 7 B. Additional images showing current evolution during these tests are shown in Appendix A.

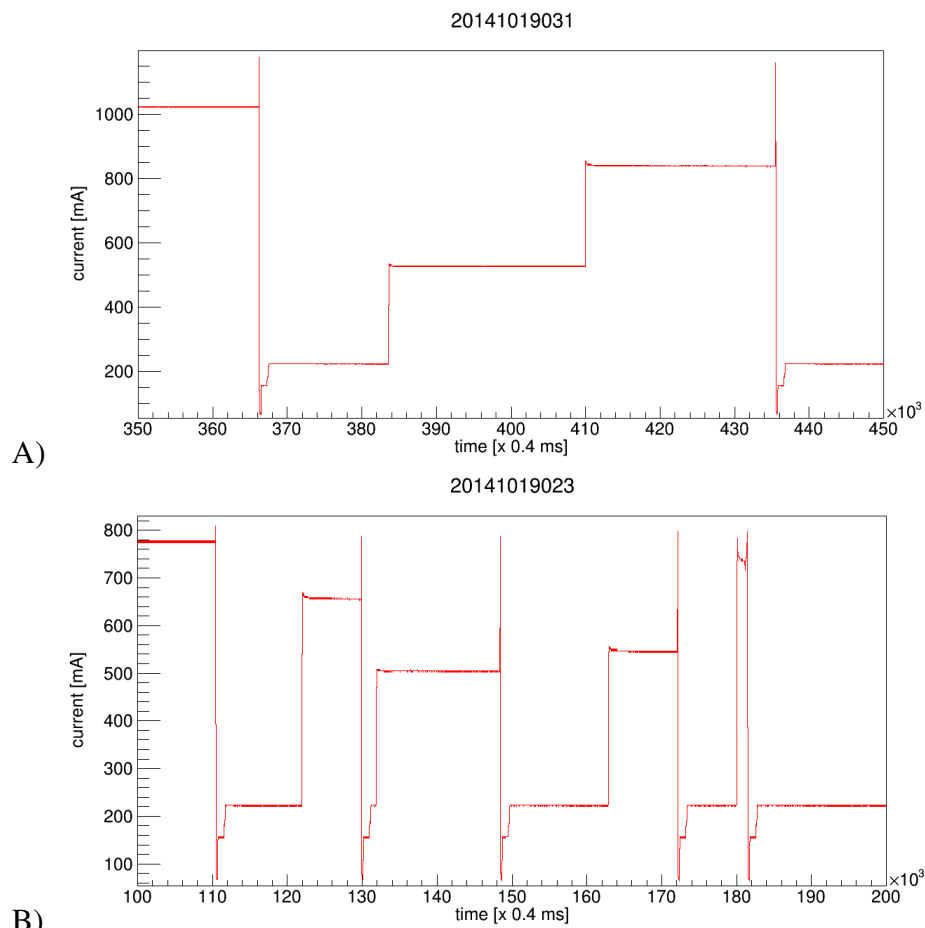


Figure 7 Current consumption associated with different current-limited latch-up events.

A clearer picture of the incremental current changes has been obtained by performing a batch analysis on all data sets⁷. Individual data sets (runs) seem to indicate a preference for current-limited latch-ups at +300mA and +500 mA (Figure 8). The sum of histograms from all runs for each sensor, shown in Figure 9, provides a less clear picture but the two above current levels still seem to be more prevalent. The wide range of the incremental current changes seems to suggest that the current-limited latch-ups can be triggered in different parts of the digital section of the chip.

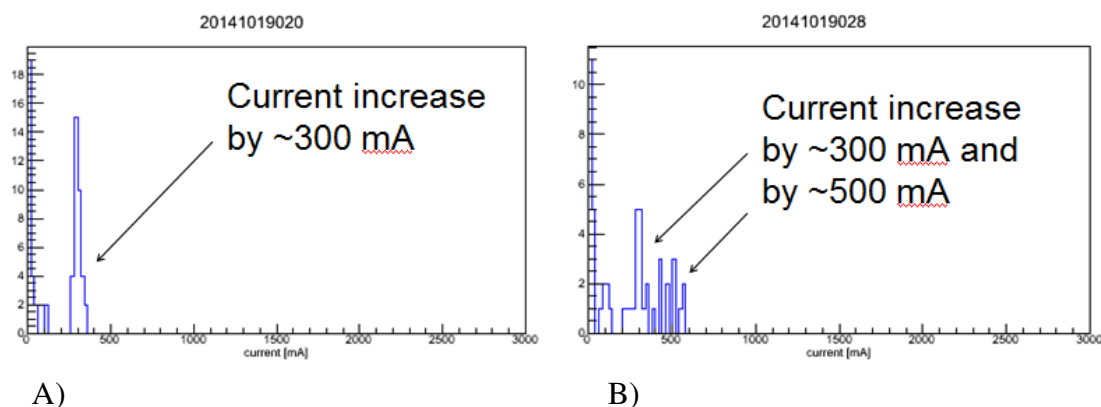


Figure 8 Current increases associated with current-limited LU events in individual runs: A) sensor 1 with over-current limit at 400 mA above the OP, B) sensor 1 with over-current limit at 800 mA above the OP.

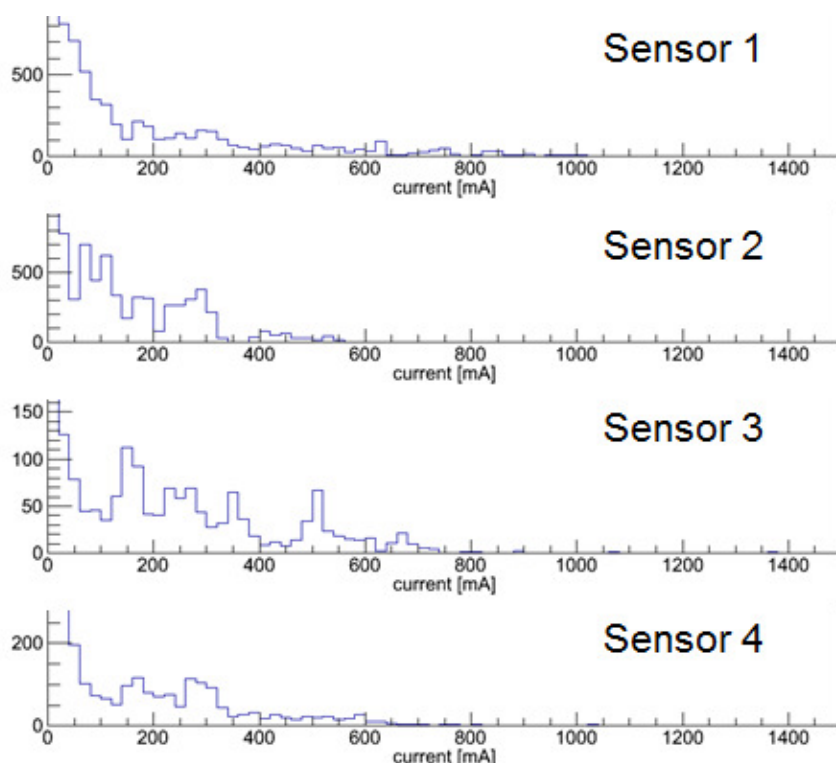


Figure 9 Current increases associated with current-limited LU events for all four tested sensors

⁷ more details on the analysis procedure can be found in:

http://rnc.lbl.gov/hft/hardware/docs/iphc_2014_12_04/LBL_IPHC_phone_meeting_4Dec2014.ppt
[LBL_IPHC_phone_meeting_4Dec2014.ppt](#)

Protons

The latch-up cross-sections measured for a single PXL sensor and a ladder at different over-current thresholds above the original operating current are summarized in Figure 10. The digital current consumption of the ladder was at the level of 900 mA until run 16 when the ladder got damaged (see Appendix B). We also observed that the current consumption in the sensor was successfully recovering to 220 mA until run 14, when it increased to 800 mA and did not decrease even after full reset.

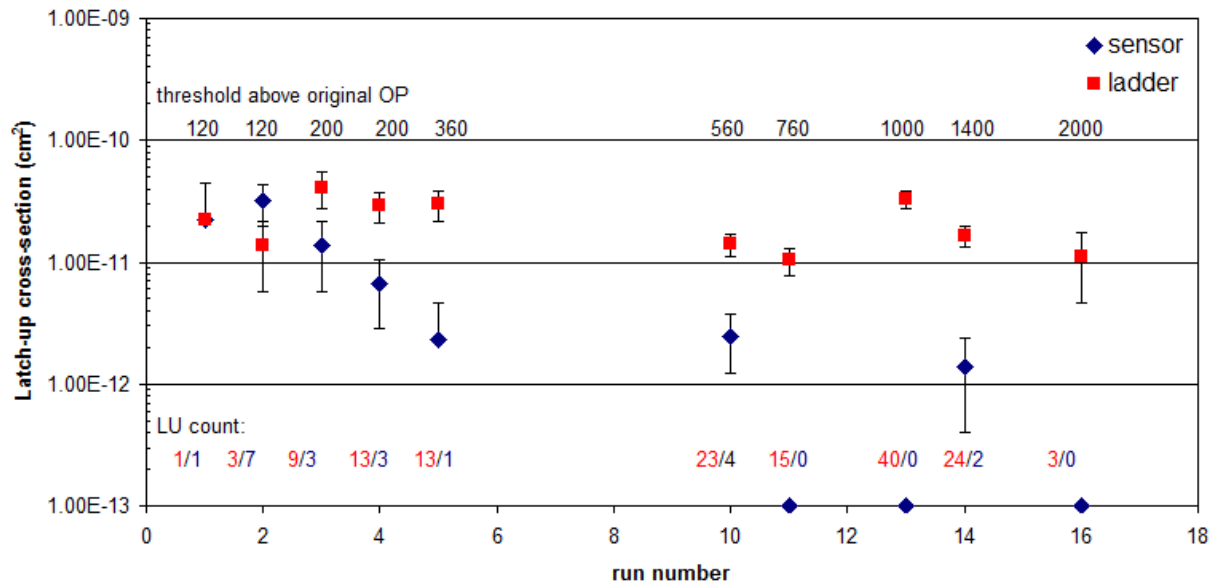


Figure 10 Latch-up cross-sections measured for 50 MeV protons.

Summary

In the series of the latch-up tests presented in this document, we tried to reproduce the type of damage observed in the PXL detector sensors during the RHIC run 14. By scanning over-current thresholds from 120 mA/300 mA up to 2 A above the operating current we managed to reproduce sensor damage. Both 50 μ m thick sensors showed damage resulting in increased operating current and visible hot spots at the over-current threshold of approximately 1A over OP. The hot spots observed on sensors damaged in the PXL detector and during this testing session are shown in Figure 11.

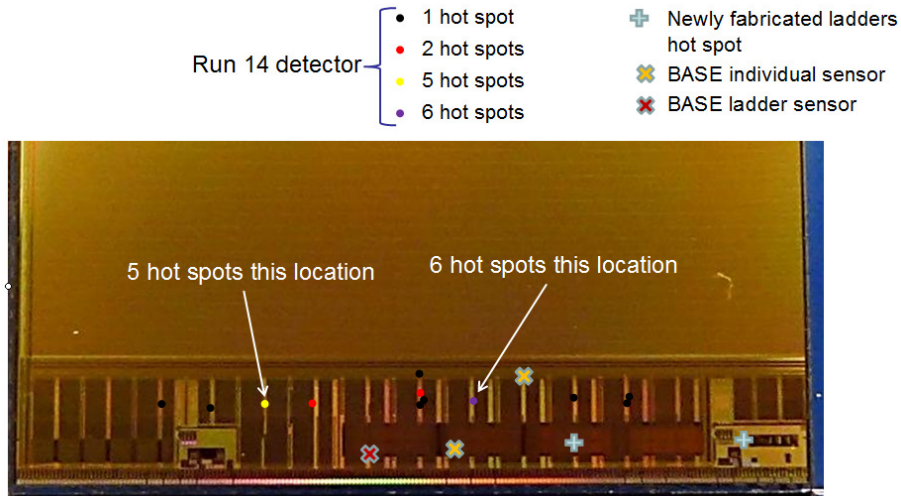


Figure 11 Distribution of hot spots on damaged PXL sensors

The 700 μm thick sensors (high and low resistivity epi) did not develop damage resulting in permanent increase of the current consumption, despite high over-current thresholds and long running times.

However, we were able to damage a thick sensor in the proton running. Before concluding on this damage, we still need to investigate in the lab environment the ladder and sensor exposed to protons. This has been impossible to do until now due to the increased radioactivity of these samples.

Overall, our test results indicated that 50 μm individual sensors and ladders appear to be susceptible to damage at a relatively high over-current threshold. However, we will never be able to measure a damage rate in any reasonable amount of time at a LU testing facility. These tests were primarily for qualitative understanding of the processes. The best measurement of a sensor damage rate in 200 GeV HI collisions is obtained from the PXL detector in run 14.

It is interesting to notice that there might be a threshold current needed for LU induced damage. PXL ladders in STAR became damaged when operated with an over-current threshold set to approximately 400 mA above the operating current of 800 mA. The individual sensors got damaged at over-current thresholds of 1000 mA above the operating current of 220 mA. In both cases the total current available in the system was at the level of ~ 1.2 A. This observation, however, might not be enough to make a definitive statement.

The behavior observed is consistent with what was observed at STAR for the run 2014 detector. The best measurement of a sensor damage rate in 200 GeV HI collisions is obtained from the PXL detector in STAR run 2014.

- 0.0025/day per sensor for LU thresholds @ 400mA above operating current
- < 0.000625 /month per sensor for LU thresholds @ 120mA above operating current

Based on this, keeping the overcurrent limits set to 120mA above the operating current for the ladders, we expect to see very little damage, likely of order < 1 -2 sensors for a 4 month running time in STAR conditions which are similar to run 2014.

Notes and Observations

During the tests we ran into problems with testing of ladder prototypes in the vacuum chamber. Debugging of the setup revealed that the exposure to the vacuum lead to the sensor ruptures and rendered ladders unusable. We conjectured that air bubbles trapped between acrylic adhesive and silicon expanded under vacuum and fractured silicon. Both ladders failed in the same way with visible fractures in one sensor on each ladder.

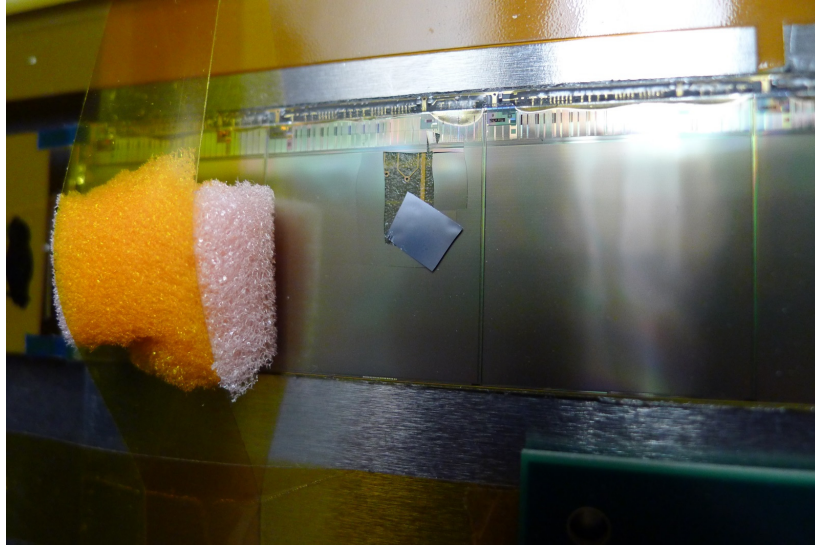


Figure 12 Exposure of the PXL ladders to a vacuum environment lead to sensor ruptures.

Appendix A

This section shows additional examples of the current consumption measured during latch-up tests with heavy ions.

Incremental current increase, hick-ups in latch-up recovery and high current consumption after the recovery can be observed in Figure 13 - Figure 16.

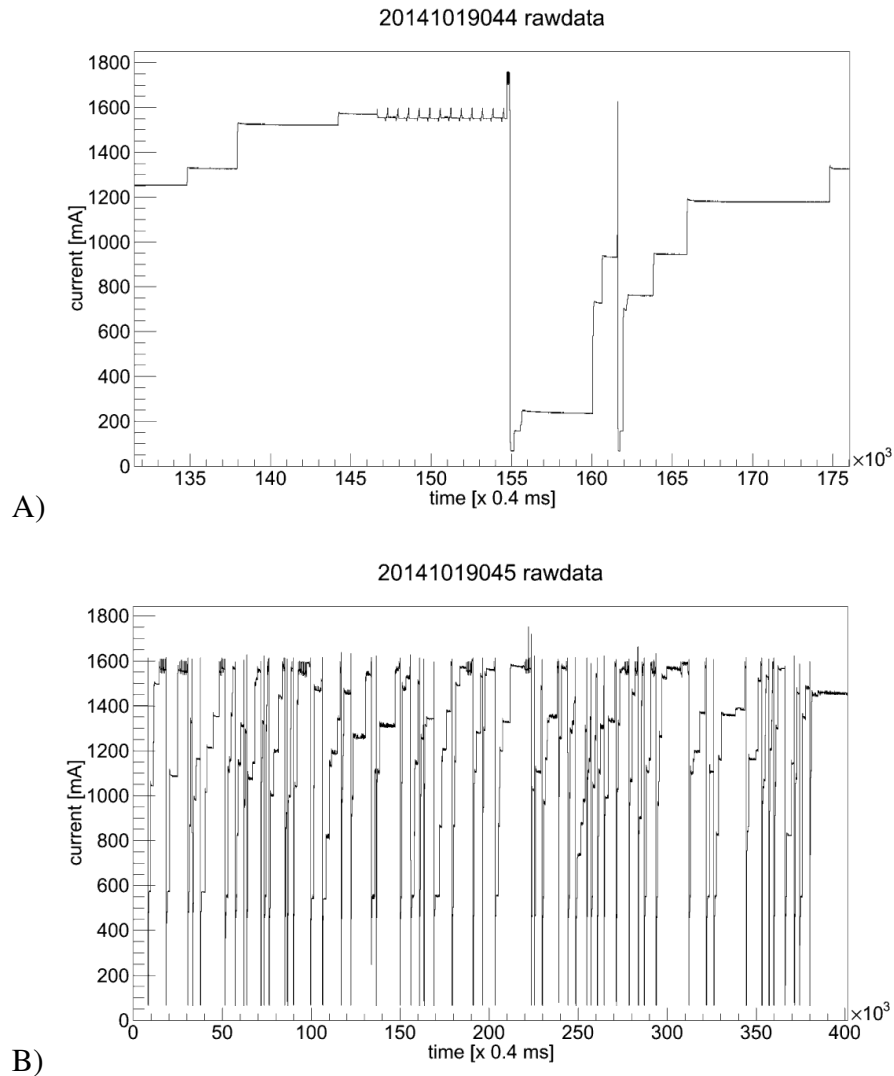


Figure 13 Current consumption for Sensor 1 (50 μ m high-res epi) at the over-current threshold set to 1.5 A above the original OP.

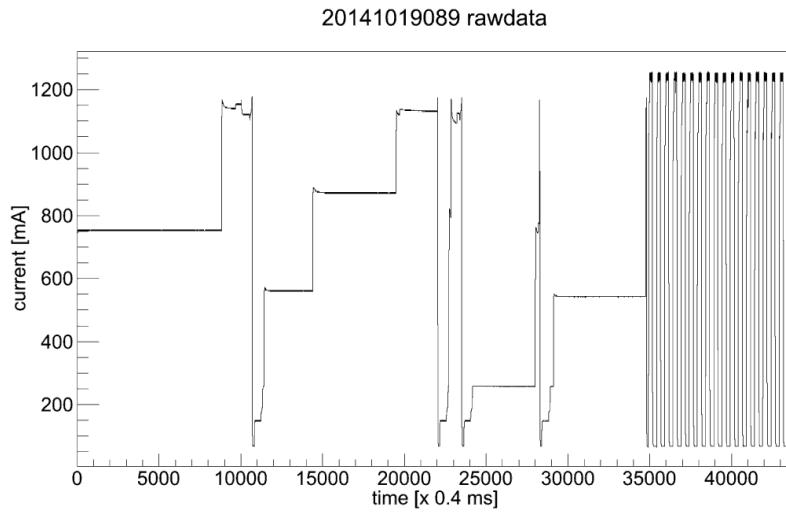


Figure 14 Current consumption for Sensor 2 (50 μ m high-res epi) at the over-current threshold set to 1.0 A above the original OP. Approximately 14 seconds into the run the sensor becomes damaged and develops high current consumption.

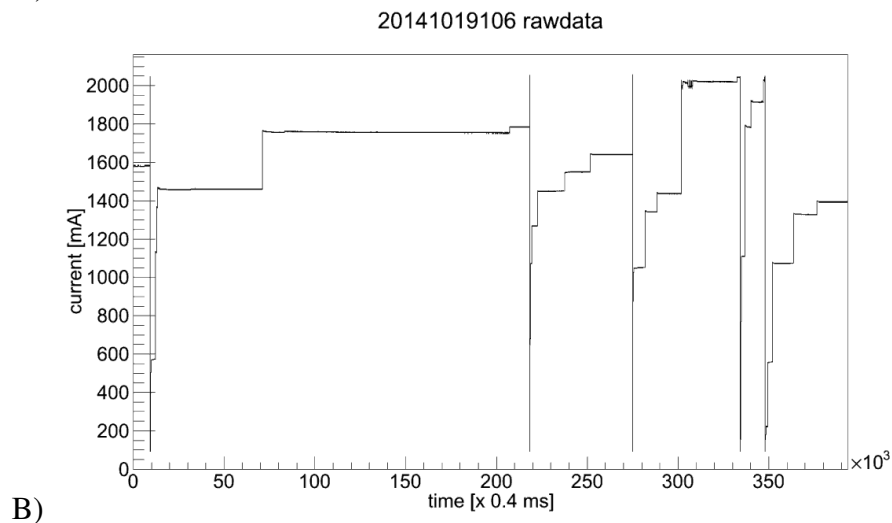
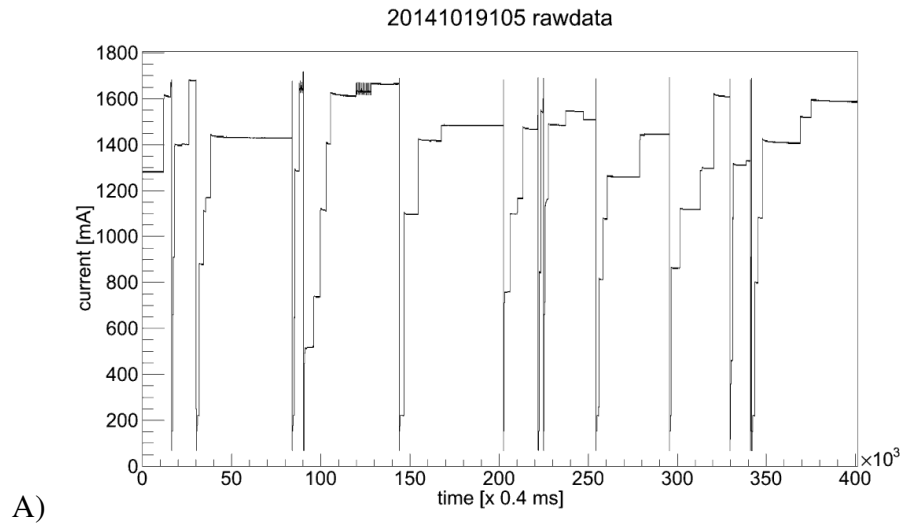


Figure 15 Current consumption for Sensor 3 (700 μ m low-res epi) at the over-current threshold set to A) 1.6 A, B) 2.0 A above the OP.

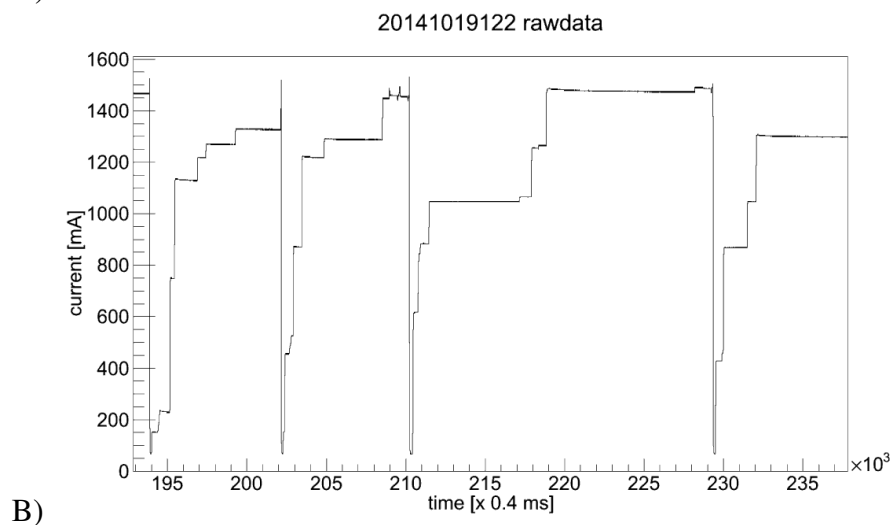
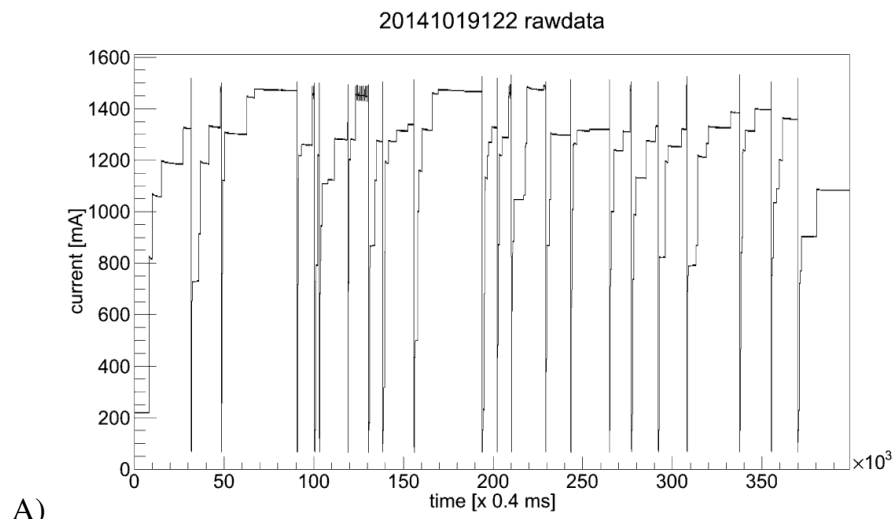


Figure 16 Current consumption for Sensor 4 (700 μ m high-res epi) at the over-current threshold set to 1.4 A above the OP.

Appendix B

The effect of the proton beam on the current consumption of the ladder and single sensor is shown in Figure 17. Both devices were configured with reasonable operating thresholds and the presence of the beam leads to intensive signal processing that results in increased power consumption.

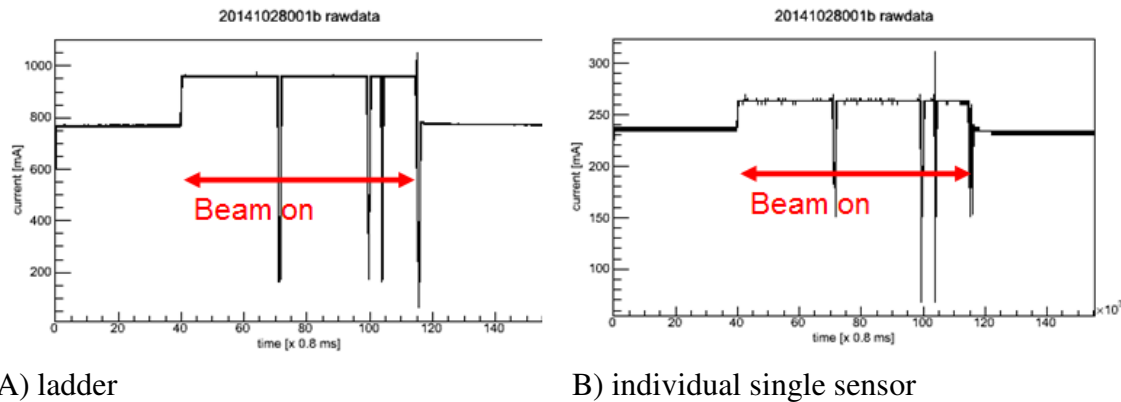


Figure 17 Increased current consumption in the ladder and individual sensor exposed to the proton beam is the result of the signal processing inside the sensors.

Examples of current consumption measured during exposure to the proton beam:

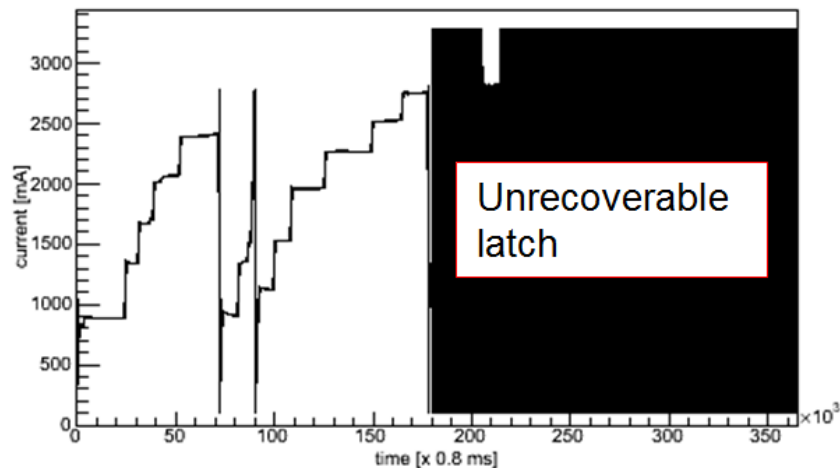


Figure 18 Evolution of the current consumption in the PXL ladder exposed to a proton beam and with the over-current threshold set to 2.0 A above the OP.

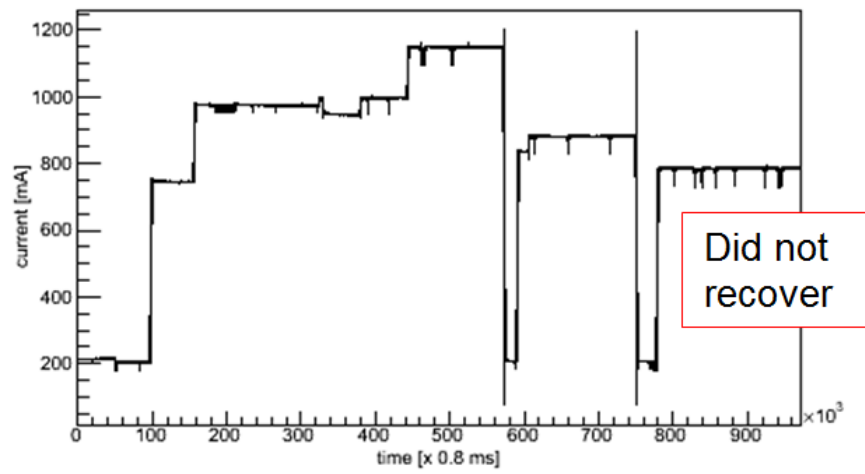


Figure 19 Evolution of the current consumption in an individual PXL sensor exposed to a proton beam and with the over-current threshold set to 1.4 A above the OP.